Engineering of Highly Luminescent Lanthanide Tags Suitable for Protein Labeling and Time-Resolved Luminescence Imaging

Nicolas Weibel,[†] Loïc J. Charbonnière,*,[†] Massimo Guardigli,[‡] Aldo Roda,*,[‡] and
Raymond Ziessel*,[†]

*Contribution from the Laboratoire de Chimie Moléculaire, Ecole de Chimie, Polymères et
Matériaux, ULP, 25 rue Becquerel, 67087 Strasbourg Cedex 02, France, and Department of
Pharmaceutical Sciences, University of Bologna, Via Belmeloro 6, 40126 Bologna, Italy*

Received December 22, 2003; E-mail: ziessel@chimie.u-strasbg.fr; aldo.roda@unibo.it

Abstract: The synthesis of a new ligand **L**H$_4$ based on a glutamic acid skeleton bis-functionalized on its nitrogen atom by 6-methylene-6′-carboxy-2,2′-bipyridine chromophoric units is described. UV−vis spectrophotometric titrations revealed the formation of 1:1 M:L complexes with lanthanide(III) cations, and complexation of **L**H$_4$ with equimolar amounts of hydrated LnCl$_3$ salts (Ln = Eu, Gd, and Tb) gave water-soluble and stable complexes of the general formula [Ln**L**(H$_2$O)]Na, which were characterized by elemental analysis, IR, UV−vis absorption spectroscopy, ^{1}H NMR (Ln = Eu), and mass spectrometry. The conditional stability constant for formation of the [Eu**L**(H$_2$O)]Na complex was determined by competitive complexation experiments to be log K = 16.5 ± 0.6 in 0.01 M TRIS/HCl buffer (pH = 7.0). In water solution, the [Eu**L**(H$_2$O)]-Na and [Tb**L**(H$_2$O)]Na complexes were highly luminescent with quantum yields of 8% and 31%, respectively, despite the presence of ca. one water molecule in the first coordination sphere of the metal ions. Activation of the appended carboxylate function of the glutamate moiety in the form of an *N*-hydroxysuccinimidyl ester allows for the covalent linking of the complexes to primary amino groups of biological compounds. Bovine serum albumin (BSA) was labeled with both Eu or Tb complexes, and the Ln−BSA conjugates were characterized by UV−vis absorption and emission spectroscopy and MALDI-TOF mass spectrometry. Labeling ratios (number of complex molecules per BSA) of ca. 8:1 and 7:1 were established for Eu−BSA and Tb−BSA, respectively. The suitability of the tagged compound for use in bioanalytical time-resolved luminescence microscopy was established by comparison with fluorescein-labeled probes.

Introduction

Recent decades have been the witness of important advances in the flourishing field of fluorescence microscopy. The large development of new fluorophores combined with technical progress for data acquisition and image processing opened up the way to new technologies with improved spatial, spectral, and temporal resolution.[1] Conventional fluorescence microscopy is sensitive enough for many applications in the biological field, in particular for the visualization of tissues or cell compartments. However, when applied to immunohistochemistry or in situ nucleic acid hybridization methods, this detection technique suffers from two main drawbacks which reduce the sensitivity of the measurements,[2] the autofluorescence of the observed samples and light scattering in the apparatus.

To avoid these disadvantages, time-resolved (also called delayed or gated) luminescence microscopy (TRLM) was proposed as an alternative to conventional fluorescence microscopy. The introduction of a suitable delay between a pulsed excitation of the sample and the measurement of the luminescence signal allows for vanishing of the short living fluorescence of the observed medium and avoidance of light scattering in the apparatus as the light source is off during the measurement of the emitted signal.[3] Unfortunately, most of the fluorophores developed so far were based on fluorescent compounds with short living excited states (a few nanoseconds), whose fluorescence would collapse as rapidly as autofluorescence does. It was thus of importance to design new luminophores with longer excited state lifetimes, such as those based on forbidden electronic transitions. Purely organic luminophores with high triplet quantum yields such as eosin or erythrosin[4] or metal complexes[5] showing ^{3}MLCT luminescence were thought to be good candidates. However, the generation of the triplet excited state is often accompanied by the photosensitization of oxygen[6] or other compounds such as diaminobenzidine (DAB).[7] Such photochemical processes severely limit the use of these luminophores in TRLM as they may lead to severe degradation of

[†] Laboratoire de Chimie Moléculaire.
[‡] University of Bologna.
(1) Tanke, H. J. *J. Microsc.* **1989**, *155*, 405.
(2) García-Parajó, M.; Verrman, J.-A.; Bouwhuis, R.; Vallée, R.; van Hulst, N. F. *Chem. Phys. Chem.* **2001**, *2*, 347.

(3) Hemmilä, I.; Harju, R. In *Bioanalytical Applications of Labeling Technologies*; Hemmilä, I.; Ståhlberg, T.; Mottram, P., Eds.; Walac Oy and EG&G Cie Pb: 1995; Chapter 5, p 83.
(4) Fleming, G. R.; Knight, A. W. E.; Morris, J. M.; Morrison, R. J. S.; Robinson, G. W. *J. Am. Chem. Soc.* **1977**, *99*, 4306.

the sample, photobleaching, and avoidance of accurate quantitative measurements.

As soon as 1978,[8] luminescent lanthanide complexes appeared as interesting labels for time-resolved applications. In the cases of europium and terbium complexes, luminescence lifetimes up to the millisecond can be obtained, leading to an improved temporal resolution in the treatment of the luminescence signal with a concomitant increase of the signal-to-noise ratio.[9] In parallel to the development of the very first lanthanide markers,[10] technical progress in time-resolved luminescence microscopy was achieved with the introduction of new devices for gated acquisition such as mechanical choppers,[11] ferro-electric liquid crystal shutters,[12] or acousto-optical modulators.[5a] Luminescent lanthanide complexes were rapidly shown to be efficient labels for cytochemistry and histochemical studies.[11b]

Despite the tremendous amount of work on luminescent lanthanide complexes,[13] only a few commercially available labels have been developed up to now.[14] The main reason for this thrift is to be found in the numerous requirements to be fulfilled by a lanthanide complex to be used in time-resolved applications.[15] In a brief survey, the complex must be stable, at least kinetically, in water; it must be soluble in aqueous media or in solvents suitable for performing its conjugation to biospecific probes; it must contain chromophoric units with large oscillator strengths at accessible wavelengths to generate the antenna effect;[16] and the intersystem crossing that leads to population of the lanthanide centered excited state after ligand excitation must be efficient, as well as must be the lanthanide centered luminescence. Finally, the synthetic procedure for obtaining the ligand must include an orthogonal function that can be activated to trigger the grafting of the lanthanide complex to the compounds to be tagged.

The two main strategies that have been developed so far to obtain stable complexes consist of either encapsulating the lanthanide cation in the well-defined macrotricyclic cavity of a cryptand[17] or including in the design of the ligand (possibly of macrocyclic- or podand-type structure) numerous anionic termini (mainly carboxylate functions[18] or phosphorus derivatives[19]) for stabilization of the complex through electrostatic interactions. Our previous work in this last direction showed us that the introduction of anionic carboxylate functions directly linked in the ortho position of a pyridyl-containing chromophore such as 2,2′-bipyridine[9,20] or pyrazolyl-pyridine[21] often gave very luminescent complexes with europium or terbium. We would now like to show how such chromophores can be combined on a glutamic skeleton to give ligand **LH₄**, which forms water-soluble, stable, and highly luminescent complexes with europium and terbium, [Ln**L**(H₂O)]Na. The noncoordinated glutamate residue can be transformed in an activated ester to form [Ln**L***(H₂O)] complexes[22] that can be easily linked to amino residues. The suitability of these complexes for labeling will be demonstrated, together with the capacity of labeled model biomolecules for use in TRLM.

Results and Discussion

Synthesis of the Ligand. Ligand **LH₄** is obtained in a seven-step synthetic protocol as described in Scheme 1.

Starting from commercially available 2-amino-6-methylpyridine **1**, a Sandmeyer reaction[23] gave 2-bromo-6-methylpyridine, which is transformed to 2-tributylstannyl-6-methylpyridine by metalation with *n*-BuLi followed by reaction with Bu₃SnCl.[24] A Stille coupling of the stannylated compound with 2,6-dibromopyridine catalyzed by [Pd(PPh₃)₄] gave 6-bromo-6′-methyl-2,2′-bipyridine.[25] A radicalar bromination with NBS/AIBN in benzene under UV irradiation gave compound **2** in 48% yield after purification.[26] Dimethyl ester glutamate, **4**, was obtained by esterification of the racemic glutamic acid hydrate **3**.[27] Reacting compound **2** in a 2.2-fold excess with **4** led to the bis *N*-alkylation in 67% yield, affording compound **5**. Due to a carboalkoxylation process[28] effected in a 50/50 (v/v) EtOH/Et₃N mixture using [Pd(PPh₃)₂Cl₂] as catalyst under a CO atmosphere, **5** is transformed into the tetraester **6** in 60% yield. A final saponification of all four esters followed by reacidification of the medium allowed for isolation of **LH₄** in the form of its trihydrochloride salt.

(5) (a) Hennink, E. J.; de Haas, R.; Verwoerd, N. P.; Tanke, H. J. *Cytometry* **1996**, *24*, 312. (b) de Haas, R. R.; van Gijlswijk, R. P. M.; van der Tol, E. B.; Veuskens, J.; van Gijssel, H. E.; Tijdens, R. B.; Bonnet, J.; verwoerd, N. P.; Tanke, H. J. *J. Histochem. Cytochem.* **1999**, *47*, 183.
(6) (a) Bedlek-Anslow, J. M.; Hubner, J. P.; Carroll, B. F.; Schanze, K. S. *Langmuir* **2000**, *16*, 9137. (b) Puklin, E.; Carlson, B.; Gouin, S.; Costin, C.; Green, E.; Ponomarev, S.; Tanji, H.; Gouterman, M. *J. Appl. Polym. Sci.* **2000**, *77*, 2795. (c) Amao, Y.; Miyashita, T.; Okura, I. *Anal. Chim. Acta* **2000**, *421*, 167.
(7) Maranto, A. R. *Science* **1982**, *21*, 953.
(8) (a) Wieder, I. In *Immunofluorescence and Related Staining Techniques*; Proceedings of the VIth International Conference on Immunofluorescence and Related Staining Techniques; Knapp, W., Holubar, K., Wick, G., Eds.; Elsevier/North-Holland Biomedical Press: Amsterdam, 1978; p 67. (b) Mayer, A.; Neuenhofer, S. *Angew. Chem., Int. Ed. Engl.* **1994**, *33*, 1044.
(9) Charbonnière, L. J.; Guardigli, M.; Cesario, M.; Roda, A.; Sabbatini, N.; Ziessel, R. *J. Am. Chem. Soc.* **2001**, *123*, 2436.
(10) (a) Hemmilä, I.; Dakubu, S.; Mukkala, V.-M.; Siitari, H.; Lövgren, T. *Anal. Biochem.* **1984**, *137*, 335. (b) Evangelista, R. A.; Pollak, A.; Allore, B.; Templeton, E. F.; Morton, R. C.; Diamandis, E. P. *Clin. Biochem.* **1988**, *21*, 173.
(11) (a) Marriott, G.; Clegg, R. M.; Ardnt-Jovin, D. J.; Jovin, T. M. *Biophys. J.* **1991**, *60*, 1374. (b) Seveus, L.; Väisälä, M.; Syrjänen, S.; Sandberg, M.; Kuusisto, A.; Harju, R.; Salo, J.; Hemmilä, I.; Kojola, H.; Soini, E. *Cytometry* **1992**, *13*, 329. (c) Marriott, G.; Heidecker, M.; Diamandis, E. P.; Yan-Marriott, Y. *Biophys. J.* **1994**, *67*, 957.
(12) Verwoerd, N. P.; Hennink, E. J.; Bonnet, J.; van der Geest, C. R. G.; Tanke, H. J. *Cytometry* **1994**, *16*, 113.
(13) See, for examples: (a) Frontiers in Lanthanide Chemistry. *Chem. Rev.* **2002**, *102*. (b) Yam, V. W.-W.; Lo, K. K.-W. *Coord. Chem. Rev.* **1998**, *184*, 157. (c) Woods, M.; Kovacs, Z.; Sherry, A. D. *J. Supramol. Chem.* **2002**, *2*, 1.
(14) Hemmilä, I.; Webb, S. *Drug Discovery Today* **1997**, *2*, 373.
(15) (a) Piguet, C.; Bünzli, J.-C. G. *Chem. Soc. Rev.* **1999**, *28*, 347. (b) Rodriguez-Ubis, J. C.; Sedano, R.; Barroso, G.; Juanes, O.; Brunet, E. *Helv. Chim. Acta* **1997**, *80*, 86.
(16) Sabbatini, N.; Guardigli, M.; Lehn, J.-M. *Coord. Chem. Rev.* **1993**, *123*, 201.

(17) (a) Alpha, B.; Lehn, J.-M.; Mathis, G. *Angew. Chem., Int. Ed. Engl.* **1987**, *26*, 266. (b) Bodar-Houillon, F.; Marsura, A. *New J. Chem.* **1996**, *20*, 1041. (c) Bazzicalupi, C.; Bencini, A.; Bianchi, A.; Giorgi, C.; Fusi, V.; Masotti, A.; Valtancoli, B.; Roque, A.; Pina, F. *Chem. Commun.* **2000**, 561.
(18) For recent examples, see: (a) Chen, J. Selvin, P. R. *J. Photochem. Photobiol., A* **2000**, *135*, 27. (b) Quici, S.; Marzanni, G.; Cavazzini, M.; Anelli, P. L.; Botta, M.; Gianolio, E.; Accorsi, G.; Armaroli, N.; Barigelletti, F. *Inorg. Chem.* **2002**, *41*, 2777. (c) Clarkson, I. M.; Beeby, A.; Bruce, J. I.; Govenlock, L. J.; Lowe, M. P.; Mathieu, C. E.; Parker, D.; Senanayake, K. *New J. Chem.* **2000**, *24*, 377. (d) Senegas, J.; Bernardinelli, G.; Imbert, D.; Bünzli, J.-C. G.; Morgantini, P.-Y.; Weber, J.; Piguet, C. *Inorg. Chem.* **2003**, *42*, 4680.
(19) For recent examples, see: (a) Griffin, J. M. M.; Skwierawska, A. M.; Manning, H. C.; Marx, J. N.; Bornhop, D. J. *Tetrahedron Lett.* **2001**, *42*, 3823. (b) Bornhop, D. J.; Hubbard, D. S.; Houlne, M. P.; Adair, C.; Kiefer, G. E.; Pence, B. C.; Morgan, D. L. *Anal. Chem.* **1999**, *71*, 2607.
(20) (a) Charbonnière, L. J.; Ziessel, R. F.; Cesario, M.; Prangé, T.; Guardigli, M.; Roda, A.; Nierengarten, H. *J. Supramol. Chem.* **2003**, *15*, 277. (b) Bünzli, J.-C. G.; Charbonnière, L. J.; Ziessel, R. *J. Chem. Soc., Dalton Trans.* **2000**, 1917.
(21) Charbonnière, L. J.; Ziessel, R. F. *Helv. Chim. Acta* **2003**, *86*, 3402.
(22) Charbonnière, L. J.; Ziessel, R. F.; Weibel, N. H.; Guardigli, M.; Roda, A. French Patent N° 03 09158.
(23) Adams, R.; Miyano, S. *J. Am. Chem. Soc.* **1954**, *76*, 3168.
(24) Jutzi, P.; Gilige, U. *J. Organomet. Chem.* **1983**, *246*, 163.
(25) Houghton, M. A.; Bilyk, A.; Harding, M. M.; Turner, P.; Hambley, T. W. *J. Chem. Soc., Dalton Trans.* **1997**, 2725.
(26) Mameri, S.; Charbonnière, L. J.; Ziessel, R. F. *Synthesis* **2003**, *17*, 2713.
(27) Weigl, M.; Wünsch, B. *Tetrahedron* **2002**, *58*, 1173.
(28) El-ghayoury, A.; Ziessel, R. *J. Org. Chem.* **2000**, *65*, 7757. (b) Charbonnière, L.; Weibel, N.; Ziessel, R. *J. Org. Chem.* **2002**, *67*, 3933.

Scheme 1 [a]
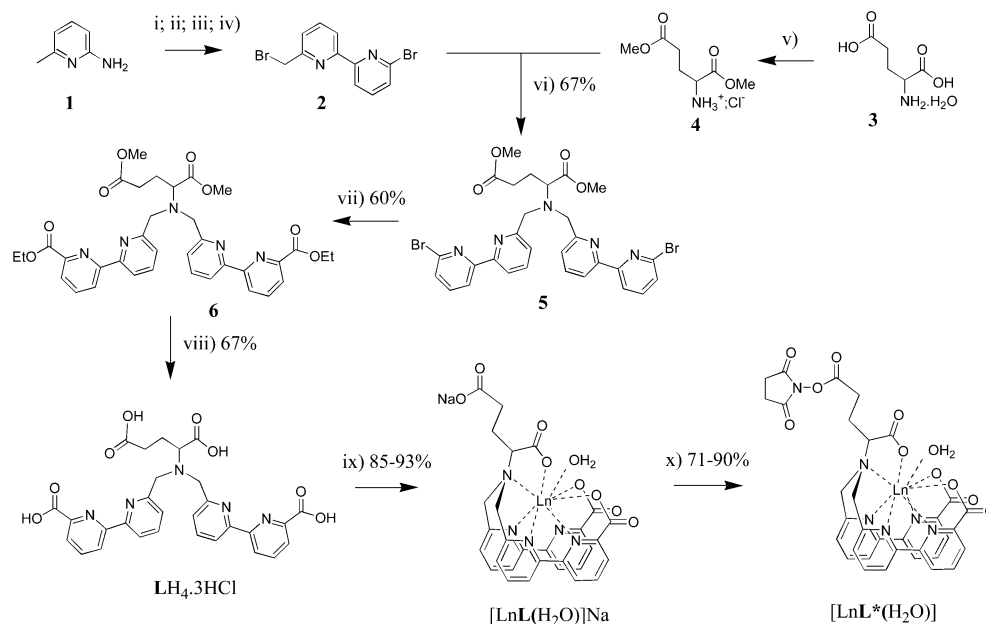
[a] (i) 48% HBr, Br$_2$, −20 °C/NaNO$_2$, NaOH. (ii) ^{n}BuLi, −78 °C/Bu$_3$SnCl. (iii) [Pd(PPh$_3$)$_4$], toluene, 110 °C, 2,6-dibromopyridine. (iv) Benzene, AIBN, NBS, *hν*. (v) TMSCl, MeOH, room temperature. (vi) Compound **2** (2.2 equiv), CH$_3$CN, K$_2$CO$_3$, 80 °C. (vii) [Pd(PPh$_3$)$_2$Cl$_2$], EtOH/Et$_3$N, CO (1 atm), 70 °C. (viii) NaOH, MeOH/H$_2$O, 70 °C/2 N HCl. (ix) LnCl$_3$·6H$_2$O, MeOH/H$_2$O, 70 °C/diluted NaOH. (x) NHS, EDCI·HCl, DMSO, room temperature.
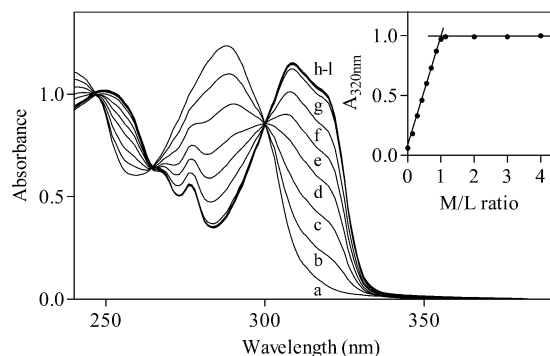

Figure 1. UV−vis spectrophotometric titration of a 5.8×10^{-5} M solution of **LH**$_4$ by EuCl$_3$·6H$_2$O in 0.01 M TRIS/HCl buffer, pH = 7.0. (a) Absorption spectra measured in correspondence with different metal/ligand ratios: (a) 0, (b) 0.14, (c) 0.29, (d) 0.43, (e) 0.57, (f) 0.71, (g) 0.86, (h) 1.0, (i) 1.14, (j) 2.0, (k) 3.0, (l) 4.0. (b) Plot of the absorbance measured at 320 nm versus added equivalents of EuCl$_3$·6H$_2$O; absorbance at this wavelength is mainly due to the lanthanide complex.

Synthesis and Characterization of the Complexes and of Their *N*-Hydroxysuccinimidyl Esters. The formation of lanthanide complexes is clearly demonstrated by UV−vis spectrophotometric titration of **LH**$_4$, effected in 0.01 M TRIS/HCl buffer (pH = 7.0) by following the variations in the UV−vis spectra of the ligand upon addition of increasing amounts of EuCl$_3$·6H$_2$O salt. Addition of aliquots of the metal immediately resulted in the displacement of the absorption maximum to lower energies, from 288 nm for the free ligand to 308 nm for 1 equiv of added lanthanide salt (Figure 1). Further addition of europium did not bring more changes. This result pointed to the formation of a single new absorbing species with a one metal to one ligand stoichiometry. In these conditions, the apparent association constants for the formation of the complexes are too high to be determined by the titration curves (Figure 1, inset) and can only be estimated as superior to 8 decimal logarithmic units. The presence in solution of a unique lanthanide-containing species is also suggested by luminescence lifetime measurements

performed upon addition of Eu^{3+} or Tb^{3+} salts. Metal luminescence decays obtained by excitation in the ligand absorption are always strictly monoexponential, and the luminescence lifetimes (see below) are independent of the amount of salt added.

Complexes of europium, gadolinium, and terbium were obtained by mixing equimolar amounts of **LH**$_4$·3HCl and LnCl$_3$· 6H$_2$O in water solutions (pH = 3−4). The mixture was then heated for an hour; the pH was made neutral before evaporation of the solvents and recrystallization of the resulting complexes.

FAB-MS spectra of the complexes were recorded in either positive or negative modes, revealing in all cases the expected molecular peak. For europium, the positive integration mode displayed [Eu**L**H] + H$^+$ as the major species with the expected isotopic pattern distribution (720.2 (80%) and 722.2 (100%)). For Tb^{3+} and Gd^{3+} ions, spectra recorded in the negative mode showed the presence of the [Ln**L**]$^-$ species (with 30% and 45% relative intensities, respectively) together with the major peak appearing at 668.2 and 667.2 *m/z* units, respectively, corresponding to the loss of a −CH$_2$COONa fragment. On the basis of the above observed formulation and due to elemental analysis and photophysical data (vide infra), the general formula was ascertained to be [Ln**L**(H$_2$O)]Na for the three complexes.

IR spectra of all complexes are very similar and point to their isostructurality in the solid state. A detailed examination of the absorption bands associated with the carboxylate groups is particularly informative (Figure 2), despite the presence of less intense perturbing bands corresponding to C=C and C=N vibrations in the same region. In the complexes, the most intense absorption band associated with the asymmetric stretching of the COO$^-$ function[29] is very broad and spans from ca. 1574 to ca. 1640 cm^{-1}. This broadness can be interpreted as the result

(29) Silverstein, R. M.; Bassler, G. C. *Identification spectrométrique des composés organiques*; Gauthier-Villars: Paris, 1968.
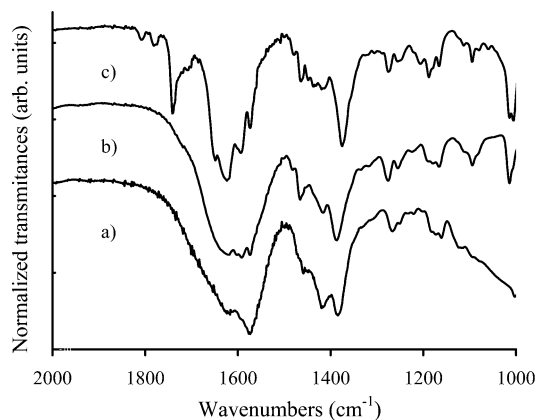
Figure 2. IR spectra of **L**Na₄ (a), [Tb**L**(H₂O)]Na (b), and [Tb**L***(H₂O)] (c) in the solid state (KBr).
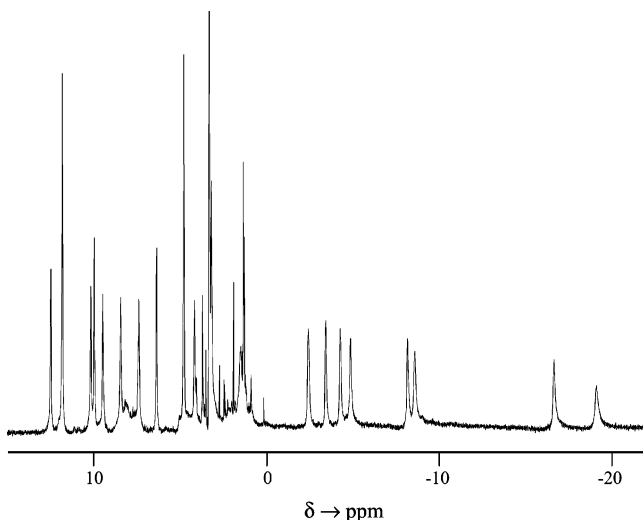
Figure 3. ¹H NMR spectrum of [Eu**L**(H₂O)]Na in CD₃OD/D₂O (with presaturation of the residual water peak).

of the different substitution on the carboxylate functions (methylene or pyridyl groups) to the various possible binding modes of the COO^- to the cation[30] and to the different counterions (Ln^{3+} or Na^+). Assuming a coordination of the lanthanide cation according to the model depicted in Scheme 1, at least three different carboxylate coordination modes should be expected, one for the COO^- linked to the bipyridyl moieties, the second for the remaining carboxylate linked to the lanthanide, and the last for the end chain COO^- assumed to be ionic with a sodium counterion. By comparison with literature data, it is likely that the absorption band of the pending carboxylate corresponds to the low energy tail of the band ($\nu_{C=O} = 1578$ cm⁻¹ for ionic sodium acetate in the solid state).[31] This attribution was further confirmed by esterification of this function (vide infra). In contrast, the symmetrical vibration mode of the carbonyl groups found around 1386 cm⁻¹ appeared as a thin absorption band with a shoulder at high energy.

The ¹H NMR spectrum of the europium complex in a CD₃OD/D₂O mixture (Figure 3) revealed the presence of 19 observable broad peaks sprayed over 40 ppm, as a result of the paramagnetic contribution of the europium atom.[32] All peaks correspond to an integration value of one proton, except that at
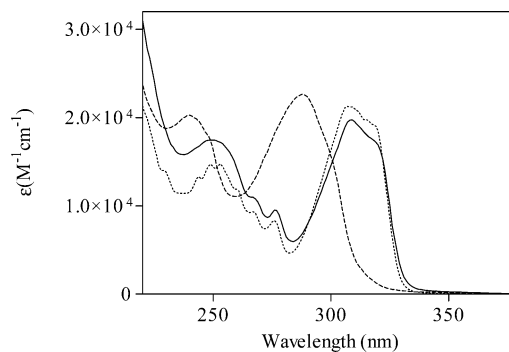
(30) Nakamoto, K. *Infrared and Raman Spectra of Inorganic and Coordination Compounds*, 4th ed.; Wiley: New York, 1986; p 231.
(31) Itoh, K.; Bernstein, H. J. *Can. J. Chem.* **1956**, *34*, 170.

Figure 4. Absorption spectrum of **L**H₄ (- - -) and [Eu**L**(H₂O)]Na (—) and metal luminescence excitation spectrum of [Eu**L**(H₂O)]Na (· · ·) in water solution.

11.81 ppm which integrates for two. The complexation of the ligand to the cation induces the formation of a single diastereomeric form of the complex. This results in the differentiation of the two bipyridyl strands and to an expected number of 21 chemically nonequivalent protons. The lacking signal may be hidden in the large peak of the residual nondeuterated water. Assuming a detection limit of 5%, ¹H NMR experiments gave an estimate of 7.3 kJ mol⁻¹ for the lower limit of the energy difference between the two diastereomeric forms.

Activation of the noncoordinated carboxylate function of the complexes was achieved with EDCI·HCl in DMSO containing *N*-hydroxysuccinimide (NHS), followed by recrystallization of the complexes. FAB-MS spectra recorded in the positive mode showed two main peaks corresponding to the [Ln**L***] + H⁺ (**L*** refers to the NHS-activated form of the ligand) species and the fragment originating from the loss of a succinimidyl fragment. The isotopic distribution observed for the molecular peak of the europium complex confirmed its mononuclear nature. The formation of the ester function in the complexes was also evidenced by the changes in the IR spectra (Figure 2). A new absorption band, attributed to the amide C=O functions of NHS, appeared at 1740 cm⁻¹. The band corresponding to the asymmetrical stretching of the COO^- functions became far thicker when compared to that of the starting complex, with a clear decrease of the intensity in the low energy tail of this absorption band (1570 cm⁻¹ region, Figure 2). This confirms the prior attribution of the spectra as corresponding to the ionic noncoordinated carboxylate function.

Photophysical Properties of the Complexes. The absorption spectra of the free ligand **L**H₄ and the [Ln**L**(H₂O)]Na complexes (Ln = Eu, Tb, or Gd) show intense absorption bands due to $\pi-\pi^*$ transitions in the ligand chromophores (Figure 4 and Table 1). The lowest-energy absorption band, which has the maximum at 288 nm in the free ligand, undergoes a red shift to 308 nm upon lanthanide complexation, as is usually observed for ligands containing bpy-type chromophores.[16,33] The maximum absorption coefficients in the complexes vary between 19 000 and 21 000 M⁻¹ cm⁻¹, in agreement with the values observed in lanthanide complexes with other ligands containing bpy-carboxylate chromophores.[9,20]

(32) (a) Bertini, I.; Lucchinat, C. *NMR of Paramagnetic Molecules in Biological Systems*; Benjamin/Cummings Publishing Co. Inc.: Menlo Park, CA, 1986. (b) Renaud, F.; Piguet, C.; Bernardinelli, G.; Bünzli, J.-C. G.; Hopfgartner, G. *J. Am. Chem. Soc.* **1999**, *121*, 9326.
(33) Sabbatini, N.; Guardigli, M.; Manet, I. In *Advances in Photochemistry*; Neckers, D. C., Volman, D. H., von Bünau, G., Eds.; John Wiley & Sons: New York, 1997; Vol. 23, p 213.

Table 1. Photophysical Properties of the Ligand **L**H$_4$ and of Its Lanthanide Complexes[a]

compound	absorption properties λ_{max} (nm), ϵ_{max} (M^{-1} cm^{-1})	metal luminescence properties[b] τ^{300K} (ms)	τ^{77K} (ms)	Φ^{300K}
LH$_4$	288, 22 300			
	239, 20 200			
[Eu**L**(H$_2$O)]Na	308, 19 700	0.62 (2.48^c)	0.8 (2.6^c)	0.08 (0.35^c)
	253, 14 400			
[Tb**L**(H$_2$O)]Na	308, 20 800	1.48 (2.53^c)	1.7 (3.1^c)	0.31 (0.53^c)
	253, 15 100			
[Gd**L**(H$_2$O)]Na	308, 19 000	—^{d}	—^{d}	—^{d}
	253, 13 600			

[a] Data obtained in water solution at room temperature, unless otherwise noted. [b] Measured upon excitation in the ligand absorption at 308 nm. [c] In D$_2$O solution. [d] No metal luminescence is observed.

As concerns the metal luminescence properties, both the Eu^{3+} and the Tb^{3+} complexes show strong metal luminescence in water solution upon excitation in the ligand absorption bands. The metal luminescence excitation spectra closely match the absorption spectra of the complexes (Figure 4), indicating that metal emission results from a ligand-to-metal energy transfer process. The emission spectra present the usual $^5D_0 \rightarrow {}^7F_J$ and $^5D_4 \rightarrow {}^7F_J$ ($J = 0-6$) transitions typical of the Eu^{3+} and Tb^{3+} ions, respectively (Figure 5).

The pattern of the Eu^{3+} complex emission spectrum, in particular the splitting into three components of the $^5D_0 \rightarrow {}^7F_1$ band (Figure 5a, inset), indicates that the first coordination sphere of the metal ion possesses a relatively low symmetry,[34] as it could be envisaged on the basis of the ^{1}H NMR data. Unfortunately, any attempt to obtain crystals suitable for X-ray analysis was unsuccessful. Both complexes exhibit long metal luminescence lifetimes in water solution (Table 1); in particular, the metal luminescence lifetime of the Tb^{3+} complex at room temperature is about 1.5 ms, a remarkably high value in comparison with those usually found in Tb^{3+} complexes of ligands containing bpy-type[33] or bpy-carboxylate[9,20] chromophores.

To investigate the reason for this photophysical behavior, we studied in detail the nonradiative decay processes of the metal emitting states. Comparison of the metal luminescence lifetimes and quantum yields measured in water and heavy water indicates that O–H vibrations make a significant contribution to the total nonradiative deactivation of the metal emitting states. Using the Horrocks and Sudnick equation[35] with the revised coefficients and the second-sphere corrections further proposed,[36,37] it was possible to establish that in both the europium and the terbium complexes the metal ion coordinates about 1.1 water molecules in solution at room temperature, a value that is in good agreement with the structure of the complex proposed in Scheme 1. In fact, lanthanide ions are known to coordinate 9–10 water molecules, and, according to the proposed structure, coordination of the lanthanide ion takes place through eight ligand atoms (i.e., three oxygen atoms from the carboxylate
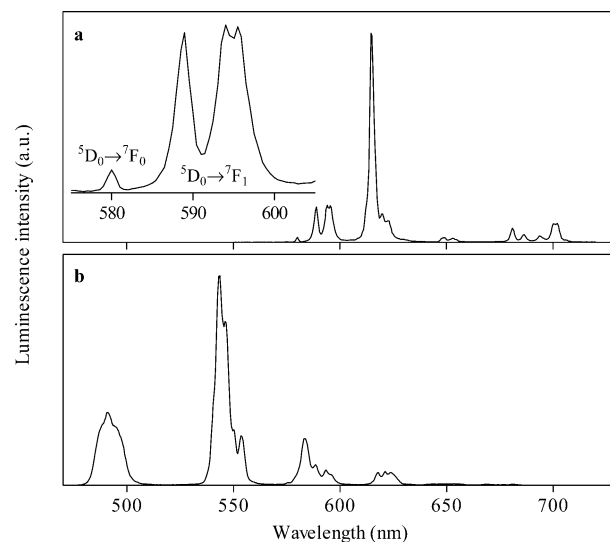
(34) Bünzli, J.-C. G. In *Lanthanide Probes in Life, Chemical and Life Sciences*; Bunzli, J.-C. G., Choppin, G. R., Eds.; Elsevier: Amsterdam, 1989; p 228.
(35) (a) Horrocks, W. De W., Jr.; Sudnick, D. R. *J. Am. Chem. Soc.* **1979**, *101*, 334. (b) Horrocks, W. De W., Jr.; Sudnick, D. R. *Acc. Chem. Res.* **1981**, *14*, 384.
(36) Beeby, A.; Clarkson, I. M.; Dickins, R. S.; Faulkner, S.; Parker, D.; Royle, L.; S. De Sousa, A.; Williams, J. A. G.; Woods, M. *J. Chem. Soc., Perkin Trans. 2* **1999**, 493.
(37) Supkowski, R.; Horrocks, W. De W., Jr. *Inorg. Chim. Acta* **2002**, *340*, 44.

Figure 5. Metal luminescence emission spectra of [Eu**L**(H$_2$O)]Na (a) and [Tb**L**(H$_2$O)]Na (b) in water solution obtained upon excitation in the main absorption band of the ligand. The inset shows an enlarged view of the emission spectrum of the [Eu**L**(H$_2$O)]Na complex in correspondence with the $^5D_0 \rightarrow {}^7F_0$ and $^5D_0 \rightarrow {}^7F_1$ transitions.

groups, and four aromatic and one aliphatic nitrogen atoms). The shielding of the metal ion by the ligand is thus quite efficient, even if the presence of a residual water molecule in the first coordination sphere of the metal ion suggests that modification of the ligand (for example, by introducing an additional metal-coordinating group in the aliphatic arm) could further improve its shielding ability, and thereby the photophysical properties of the lanthanide complexes. Comparison of the photophysical behavior of the Eu^{3+} and Tb^{3+} complexes in water and heavy water clearly shows that the importance of solvent-induced nonradiative decay processes depends on the nature of the lanthanide ion. In fact, in going from heavy water to water solutions, the metal luminescence lifetime and quantum yield decrease much more for the Eu^{3+} than for the Tb^{3+} complex, because of the lower susceptibility of the Tb^{3+} ion to solvent-induced nonradiative decay processes.

Thermally activated back-energy transfer processes from the metal emitting state to ligand excited states often represent one of the most important nonradiative decay processes in lanthanide complexes, particularly the Tb^{3+} ones.[33] However, comparison of the lifetime values obtained at 300 and 77 K demonstrates that in both the [Eu**L**(H$_2$O)]Na and the [Tb**L**(H$_2$O)]Na complexes such processes only play a minor role in the decay of the metal emitting state. Low-temperature ligand phosphorescence measurements performed on the [Gd**L**(H$_2$O)]Na complex allowed one to estimate that in the lanthanide complexes the ligand triplet excited state lies at about 22 100 cm^{-1}, that is, 1700 cm^{-1} above the Tb^{3+} metal emitting state. Although the energy gap between these levels is slightly below the limiting value of 1850 cm^{-1} proposed by Latva and co-workers,[38] its value can well account for the low efficiency of thermally activated nonradiative decay processes and thus for the long luminescence lifetimes of the Tb^{3+} complex.

Both complexes showed high metal luminescence quantum yields in water solution upon excitation into the ligand absorp-

(38) Latva, M.; Takalo, H.; Mukkala, V.-M.; Matachescu, C.; Rodriguez-Ubis, J. C.; Kankare, J. *J. Lumin.* **1997**, *75*, 149.

tion bands (Table 1), and the luminescence quantum yield of the Tb^{3+} complex is, to our knowledge, the highest value obtained up to now for complexes with bpy-type ligands.[33] The high quantum yields of the complexes are due to the high efficiency of both the energy transfer process from the ligand excited states to the metal emitting state (which generates the antenna effect) and the lanthanide luminescence. Assuming that the decay of the metal emitting state at 77 K in D_2O is purely radiative, ligand-to-metal energy transfer and metal luminescence efficiencies can be estimated from the experimental metal luminescence lifetimes and quantum yields. As concerns the efficiency of the ligand-to-metal energy transfer process, values of 0.65 and 0.36 are obtained for the Tb^{3+} and Eu^{3+} complexes, respectively. Metal luminescence is also an efficient process, especially in the Tb^{3+} complex: in water, the efficiency of metal luminescence is 0.49 and 0.24 for the Tb^{3+} and Eu^{3+} complexes, respectively. Overall, the excellent photophysical properties of the europium and terbium complexes here presented, as well as those of the lanthanide complexes of related ligands,[9] demonstrate the suitability of the bpy-carboxylate chromophore as a building block for the design of ligands capable of forming stable and strongly luminescent lanthanide complexes.

Stability of the Lanthanide Complexes. The high stability of a lanthanide complex is a necessary prerequisite for its use in biological media, that is, in the presence of negatively charged groups such as phosphate or carboxylate, able to strongly bind to lanthanide ions. The lanthanide complexes of ligand $\mathbf{LH_4}$ were found to be stable for several days in common buffers used in bioanalytical chemistry, including 0.01 M TRIS/HCl, pH = 7.0, and PBS (phosphate buffer saline: 0.02 M Na_2HPO_4/NaH_2PO_4 buffer with 0.15 M NaCl, pH = 7.4). The photophysical properties of the complexes in buffer solutions are almost identical to those obtained in pure water.

The conditional stability constant $K_{cond,L}$ for the formation of the europium complex with $\mathbf{LH_4}$ in water was measured at 25 °C in 0.01 M TRIS/HCl (pH = 7.0) following a procedure based on the competition between two ligands, one of which (EDTA) has a known stability constant for formation of its Eu^{3+} complex.[39] In such a way, the ratio between the conditional stability constants of the two complexes can be determined, from which the unknown stability constant is calculated. For the $[Eu\mathbf{L}(H_2O)]Na$ complex, log $K_{cond,Eu\mathbf{L}}$ was measured to be 16.5 ± 0.6 (to be compared to log $K_{cond,EDTA} = 14.1$),[39,40] showing the ligand forms lanthanide complexes that are more stable than those with EDTA at physiological pH. As concerns the thermodynamic stability constant for the formation of the $[Eu\mathbf{L}(H_2O)]Na$ complex, it should be evaluated from $K_{cond,Eu\mathbf{L}}$ using the stepwise protonation constants of the ligand L, which were not yet determined. However, the high value of the conditional stability constant of the lanthanide complexes of ligand $\mathbf{LH_4}$ suggests that these complexes are suitable for application in bioanalytical assays, as well as in immunohistochemical and in situ hybridization experiments.

Synthesis and Characterization of Conjugates with BSA. The *N*-hydroxysuccinimidyl (NHS) ester is probably the most common functional group used in bioanalytical chemistry for the covalent coupling of labels to the primary amino groups
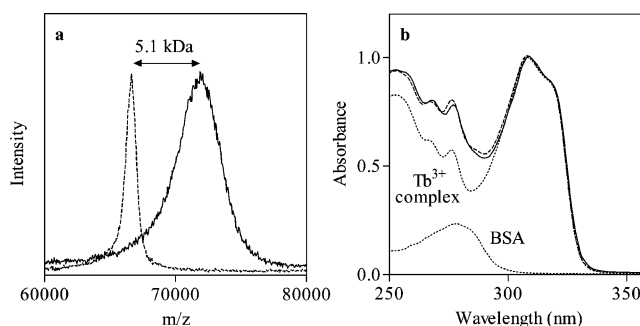

Figure 6. Characterization of the Tb−BSA conjugate by mass spectrometry and UV−vis absorption spectroscopy. (a) MALDI-TOF mass spectra of BSA (- - -) and Tb−BSA (—). (b) Experimental UV−vis absorption spectrum of Tb−BSA (—) and theoretical absorption spectrum (- - -) obtained as the sum of individual BSA and Tb^{3+} chelate spectra (shown as dotted lines). The best fitting of the experimental spectrum was obtained assuming a ca. 8.5:1 labeling ratio.

(usually lysine residues) of biomolecules such as albumins, enzymes, and immunoglobulins.[41] The coupling reaction with NHS esters is performed under mild alkaline conditions, in which the ester reacts specifically with primary amino groups. In addition, it is not harmful to biologically active compounds, and high reaction yields can be achieved, minimizing protein denaturation.

The suitability of the $[Eu\mathbf{L}^*(H_2O)]$ and $[Tb\mathbf{L}^*(H_2O)]$ NHS activated esters for protein labeling was demonstrated using bovine serum albumin (BSA) as a model protein. BSA is known to possess 59 lysine residues which can potentially react with NHS esters.[42] However, to avoid an excessive labeling of the protein, the conjugation reaction was carried out using a 30:1 label/protein molar ratio. In fact, a high degree of labeling will increase the signal-to-mass ratio of the conjugate, and thus its detectability, but it could also affect the biological activity of the labeled biomolecule (for example, the recognition ability of an antibody can be impaired). In addition, extensive labeling may give rise, as observed for fluorescein-labeled compounds, to self-quenching of the label's emission. Characterization of the conjugates in terms of label/protein molar ratio was performed by means of MALDI-TOF mass spectrometry and UV−vis absorption spectroscopy.

The comparison of the molecular mass of the lanthanide labeled BSA (72.3 and 71.7 kDa for the Eu− and Tb−BSA conjugates, respectively) with that of the starting protein (66.6 kDa) allowed one to establish that the mean number of lanthanide labels per BSA molecule is 8.1 for Eu−BSA and 7.3 for Tb−BSA (Figure 6a). These findings are in reasonable agreement with the labeling ratios measured by UV−vis spectroscopy (Figure 6b), under the assumption that (i) the absorption spectrum of the conjugate is the sum of the absorption spectra of BSA and of the lanthanide label and (ii) these spectra coincide with those of the free species. Conjugation reaction was thus characterized by a yield of ca. 25%, which could presumably be improved through further optimization of the conjugation protocol.

As concerns metal luminescence, both protein conjugates maintain the excellent photophysical properties of the $[Eu\mathbf{L}(H_2O)]$-Na and $[Tb\mathbf{L}(H_2O)]Na$ complexes. The conjugates, particularly

(39) Wu, S. L.; Horrocks, W. De W., Jr. *Anal. Chem.* **1996**, *68*, 394.
(40) Smith, R. M.; Martell, A. E. *Critical Stability Constants*; Plenum Press: New York, 1974; Vol. 1, p 204.
(41) Hermanson, G. T. *Bioconjugate Techniques*; Academic Press: New York, 1996.
(42) Goodno, C. C.; Swaisgood, H. E.; Catignani, G. L. *Anal. Biochem.* **1981**, *115*, 203.
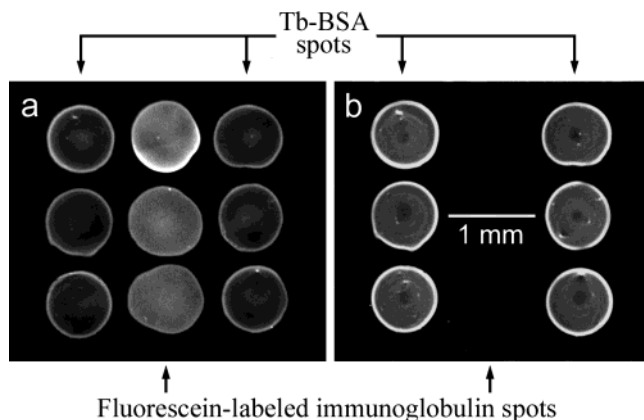
Figure 7. Microscope luminescence imaging of a 3 × 3 array of spots containing Tb−BSA (left and right columns) or a fluorescein-labeled rabbit immunoglobulin (middle column). Images were taken in prompt (a) and time-resolved (b) fluorescence mode.

the Eu^{3+} one, show polyexponential metal luminescence decays, presumably because the label molecules bound to the protein lie in different surrounding environments. It is interesting to note that the mean metal luminescence lifetime of the Eu−BSA conjugate (1.10 ms) is significantly longer than that of the [Eu**L**(H_2O)]Na complex. The opposite behavior is shown by Tb−BSA, for which the mean metal luminescence lifetime (1.31 ms) is slightly shorter than that of [Tb**L**(H_2O)]Na complex. As concerns the metal luminescence quantum yields of the conjugates, their values present a trend similar to that of the luminescence lifetimes: the quantum yields of Eu−BSA (0.13) and Tb−BSA (0.28) are, respectively, significantly higher and slightly lower than those of the [Ln**L**(H_2O)]Na complexes. As a tentative explanation, the increase in the luminescence lifetime and quantum yield of the Eu−BSA conjugate can be attributed to partial replacement of water in the first coordination sphere of the Eu^{3+} ion by other metal-coordinating groups belonging to the surface of the protein, thereby resulting in a reduced efficiency of solvent-induced nonradiative deactivation processes. The Tb−BSA conjugate should undergo the same phenomenon; however, it has been already observed that changes in the metal coordination sphere in Tb^{3+} complexes (due, for example, to coordination of anions to the metal ion) can have effects on the photophysical properties that cannot be explained by simply considering the removal of coordinated water molecules.[43]

Imaging Experiments on the Tb−BSA Conjugate. The Tb−BSA conjugate was used as a model to demonstrate the suitability of the lanthanide complexes here presented as labels for time-resolved luminescence microscopy. TRLM experiments (Figure 7) were carried out on spots (diameter ≈ 800 μm) of Tb−BSA containing 2−3 ng of labeled protein, which were imaged together with spots containing similar amounts of fluorescein-labeled rabbit immunoglobulins.

As expected, both fluorescein-labeled antibody and Tb−BSA spots appeared in the prompt fluorescence image (Figure 7a), while the short-lifetime emission of the fluorescein-labeled antibody completely disappeared in the image acquired in the time-resolved fluorescence mode (Figure 7b). Quantitative analysis of the signals demonstrates that time-resolved fluores-

cence measurements provide for a more than 1000-fold increase in the lanthanide label/fluorescein emission ratio in comparison to the prompt fluorescence measurement. These findings suggest that, due to the long lifetimes and high quantum yields of the lanthanide luminescence, biospecific probes labeled with the lanthanide chelates described in this paper will allow the development of assays relying on time-resolved luminescence imaging measurements with efficient suppression of the sample background fluorescence.

Conclusion

The introduction of two bipyridine carboxylic acid arms on a glutamic skeleton led to the easy synthesis of ligand **L**H_4 that has a high affinity toward lanthanide cations. The Eu^{3+} and Tb^{3+} lanthanide complexes thereby obtained are highly luminescent in water at neutral pH, despite the presence of a water molecule in the first coordination sphere of the cations. IR data showed that the propionate function on the glutamic residue remained uncoordinated, which allows for its esterification into an activated *N*-hydroxysuccinimidyl ester. In this form, the complex can be covalently linked to amino functions present on protein as evidenced by reaction with BSA.

This new family of lanthanide tags offers significant improvements as compared to conventional organic fluorescent markers or to the previously known compounds. Among those, the ease of synthesis make it very attractive for a broad scope of applications. The large Stokes' shift (more than 14 000 and 16 000 cm^{-1}, respectively, for the most intense emission bands of terbium and europium upon excitation in the bipyridine moieties) facilitates spectral discrimination when the tag is simply used as a fluorescent marker. Simple optical cutoff filters are necessary, while organic fluorophores often require expensive band-pass filters with losses in the out-of-the-band emission signals. The long-living excited states allow for temporal resolution with a concomitant improvement in the signal-to-noise ratio.[9] The tags are thereby particularly well suited for time-resolved applications such as time-resolved fluoroimmunoassays (TRFIA),[44] time-resolved luminescence microscopy and lifetime mapping,[45] and time-resolved fluorescence energy transfer experiments.[46] Ongoing studies are aimed at labeling biospecific molecules, such as antibodies, for the development of sensitive immunohistochemical and in situ hybridization methods on tissues and single cells or other bioanalytical methods based on time-resolved luminescence measurements. The signal/mass ratio of the probe could be further increased by developing amplified detection systems, such as those based on the biotin−streptavidin interaction that were previously used in conjunction with luminescent lanthanide chelates (even if characterized by low luminescence quantum yield).[47] Finally, the presence of a water molecule directly coordinated to the first coordination sphere of the cation opens further interesting perspectives for the development of gadolinium-based tags and their use as relaxation agents for functional magnetic resonance imaging.

(43) Sabbatini, N.; Guardigli, M.; Lehn, J.-M.; Mathis, G. *J. Alloys Compd.* **1992**, *180*, 363.

(44) Mathis, G. Biological Applications of Rare Earth Cryptates. In *Rare Earth, Cursos de Verano de El Escorial*; Saez, R., Caro, P., Eds.; Editorial Complutense: 1998; pp 285−297.
(45) Beeby, A.; Botchway, S. W.; Clarkson, I. M.; Faulkner, S.; Parker, A. W.; Parker, D.; Williams, J. A. G. *J. Photochem. Photobiol., B* **2000**, *57*, 83.
(46) (a) Blomberg, K.; Hurskainen, P.; Hemmilä, I. *Clin. Chem.* **1999**, *45*, 855. (b) Tsuji, A.; Sato, Y.; Hirano, M.; Suga, T.; Koshimoto, H.; Taguchi, T.; Ohsuka, S. *Biophys. J.* **2001**, *81*, 501.
(47) (a) Quin, Q.-P.; Lövgren, T.; Petterson, K. *Anal. Chem.* **2001**, *73*, 1521. (b) Scorilas, A.; Diamandis, E. P. *Clin. Biochem.* **2000**, *33*, 345.

Experimental Section

Solvents and raw materials were of analytical grade and were used as received. An exception was acetonitrile, which was filtered over activated alumina (Merck, Darmstadt, Germany) and distilled from P_2O_5 under an argon atmosphere immediately prior to use.[48] Compounds **2**[26] and **4**[27] were synthesized according to literature procedures. Fluorescein-labeled rabbit immunoglobulin, 2.3:1 (fluorescein/antibody) labeling ratio, was purchased from Dako (Glostrup, Denmark).

^{1}H NMR (200 and 300 MHz) and ^{13}C NMR (50 and 75 MHz) spectra were recorded with Brücker AC200 and AC300 spectrometers, using perdeuterated solvents as internal standards. FT-IR spectra were obtained from KBr pellets on a Nicolet 210 spectrometer. Fast-atom bombardment (FAB) mass spectra were recorded using *meta*-nitrobenzyl alcohol as matrix. Absorption spectra were recorded on Uvikon 933 (Kontron Instrument, Milano, Italy) and Cary 50 (Varian, Inc., Palo Alto, CA) spectrophotometers. Metal luminescence emission and excitation spectra and metal luminescence lifetimes were measured using a Varian Eclipse spectrofluorimeter. Metal luminescence quantum yields were measured using the procedure described by Haas and Stein,[49] using as standards $Ru(bpy)_3^{2+}$ ($\Phi = 0.028$ in aerated water)[50] for Eu^{3+} and quinine sulfate ($\Phi = 0.546$ in 1 N H_2SO_4)[51] for Tb^{3+} as reference. MALDI-TOF mass spectrometry analysis was performed on a Voyager-DE PRO mass spectrometer (Applied Biosystems, Foster City, CA) using α-cyano-4-hydroxycinnamic acid as matrix.

Imaging experiments were performed using an epifluorescence microscope (Olympus BX 60, Olympus Optical, Tokyo, Japan) modified for time-resolved luminescence measurements.[52] The microscope was equipped with an auxiliary pulsed excitation source (L7684 Xenon flash lamp, Hamamatsu Photonics K. K., Shimokanzo, Japan) triggered by an optical chopper located in the light emission pathway. The delay between sample excitation and luminescence measurement was controlled by modifying the phase or the speed of the chopper. The signal was acquired by means of an ultrasensitive, cryogenically cooled CCD camera (LN/CCD, Princeton Instruments, Roper Scientific, Trenton, NJ). Tb−BSA and fluorescein-labeled rabbit immunoglobulin spots (diameter ≈ 800 μm) were deposited on silanized microscope glass slides (Sigma-Aldrich Co., St. Louis, MO) by means of a glass slide microarrayer (BioGene, Kimbolton, UK); the amount of labeled protein was evaluated from the volume of solution deposited in each spot (∼3 nL). Time-resolved luminescence images were acquired with a 0.5 ms delay between the excitation of the sample and the acquisition of the luminescence signal, while no delay was used for the acquisition of prompt fluorescence images; to obtain a good signal-to-noise ratio, the overall acquisition time for each image was 60 s. Quantitative evaluation of the luminescence images was done using the Metamorph image analysis software package (Universal Imaging Corp., Downington, PA).

Synthesis of the Ligand. *N*,*N*-[(6′-Bromo-2,2′-bipyridine-6-yl)-methyl]glutamic Acid Dimethyl Ester, 5. In a Schlenk tube under argon were dissolved glutamic acid dimethyl ester hydrochloride **4** (470 mg, 2.22 mmol) and anhydrous K_2CO_3 (1.23 g, 8.90 mmol) in 100 mL of dry acetonitrile. The solution was heated to 80 °C for 30 min, and compound **2** (1.60 g, 4.88 mmol) was added. The solution was heated to 80 °C for 23 h. The mixture was evaporated to dryness, and the solid residue was partitioned between 100 mL of CH_2Cl_2 and 20 mL of water. The aqueous phase was further extracted twice with 20 mL of CH_2Cl_2, and the combined organic layers were dried over MgSO$_4$,

filtered, and evaporated to dryness. The resulting solid was purified by flash column chromatography (SiO$_2$, 100/0 to 97/3 CH_2Cl_2/MeOH) to give compound **5** (995 mg, 67%) as a pale yellow solid. $R_f = 0.34$ (SiO$_2$, 98/2 CH_2Cl_2/MeOH). ^{1}H NMR (CDCl$_3$, 200 MHz): δ 2.06− 2.20 (m, 2H), 2.39−2.68 (m, 2H), 3.50 (s, 3H), 3.54−3.62 (m, 1H), 3.76 (s, 3H), 3.99−4.16 (m, 4H), 7.43−7.48 (m, 4H), 7.63 (t, 2H, ^3J = 8.0 Hz), 7.71 (t, 2H, ^3J = 8.0 Hz), 8.23 (d, 2H, ^3J = 8.0 Hz), 8.39 (d, 2H, ^3J = 8.0 Hz). ^{13}C NMR (CDCl$_3$, 50 MHz): δ 24.8, 30.3, 51.5, 57.2, 62.1, 119.6, 119.7, 123.5, 127.8, 137.3, 139.1, 141.5, 153.8, 157.4, 159.1, 173.1, 173.4. FAB$^+$/MS: 670.2 ([3 + H]$^+$, 100%). Anal. Calcd for $C_{29}H_{27}N_5O_4Br_2$: C, 52.04; H, 4.07; N, 10.46. Found: C, 51.81; H, 3.85; N, 10.19.

***N*,*N*-[(6′-Carboethoxy-2,2′-bipyridine-6-yl)methyl]glutamic Acid Dimethyl Ester, 6.** A solution of compound **5** (995 mg, 1.49 mmol) and [Pd(PPh$_3$)$_2$Cl$_2$] (150 mg, 0.21 mmol) in a mixture of 50 mL of ethanol and 50 mL of triethylamine was heated at 70 °C for 15 h, under a continuous flow of CO at atmospheric pressure. The solution was evaporated to dryness, and the resulting solid was dissolved in 100 mL of CH_2Cl_2 and filtered over Celite. The organic layer was washed with 20 mL of water, and the aqueous layer was extracted twice with 20 mL of CH_2Cl_2. The combined organic layers were dried over MgSO$_4$, filtered, and evaporated to dryness. The resulting solid was purified by flash column chromatography (SiO$_2$, 99/1 to 90/10 CH_2Cl_2/MeOH) to give compound **6** (588 mg, 60%) as a slightly orange oil. $R_f = 0.30$ (SiO$_2$, 95/5 CH_2Cl_2/MeOH). ^{1}H NMR (CDCl$_3$, 200 MHz): δ 1.46 (t, 6H, ^3J = 7.0 Hz), 2.06−2.19 (m, 2H), 2.38−2.65 (m, 2H), 3.49 (s, 3H), 3.55−3.63 (m, 1H), 3.76 (s, 3H), 4.02−4.19 (m, 4H), 4.48 (q, 4H, ^3J = 7.0 Hz), 7.47 (d, 2H, ^3J = 8.0 Hz), 7.75 (t, 2H, ^3J = 8.0 Hz), 7.92 (t, 2H, ^3J = 8.0 Hz), 8.10 (d, 2H, ^3J = 8.0 Hz), 8.40 (d, 2H, ^3J = 8.0 Hz), 8.62 (d, 2H, ^3J = 8.0 Hz). ^{13}C NMR (CDCl$_3$, 50 MHz): δ 14.3, 24.8, 30.4, 51.5, 57.2, 61.8, 62.0, 119.9, 123.5, 124.2, 124.8, 137.3, 137.7, 147.8, 154.6, 156.5, 159.0, 165.4, 173.2, 173.5. FAB$^+$/MS: 656.2 ([4 + H]$^+$, 100%). Anal. Calcd for $C_{35}H_{37}N_5O_8$: C, 64.11; H, 5.69; N, 10.68. Found: C, 64.07; H, 5.55; N, 10.53.

***N*,*N*-[(6′-Carboxy-2,2′-bipyridine-6-yl)methyl]glutamic Acid Tri-hydrochloride LH$_4$·3HCl.** A solution of compound **6** (588 mg, 0.90 mmol) and NaOH (144 mg, 3.60 mmol) in a mixture of 50 mL of methanol and 15 mL of water was heated to 70 °C for 5 h. The solution was evaporated to dryness, and the resulting solid was dissolved in 10 mL of water. 2 N HCl was slowly added until a consequent precipitate appeared (pH = 2−3). Upon centrifugation, **L**H$_4$·3HCl (411 mg, 67%) was isolated as a pale yellow powder. ^{1}H NMR (CD$_3$OD, 300 MHz): δ 2.26−2.48 (m, 2H), 2.80−2.84 (m, 2H), 3.95−3.99 (m, 1H), 4.53− 4.81 (m, 4H), 7.47 (d, 2H, ^3J = 7.5 Hz), 7.63 (t, 2H, ^3J = 8.0 Hz), 7.90 (t, 2H, ^3J = 8.0 Hz), 8.02 (d, 2H, ^3J = 7.5 Hz), 8.42 (d, 2H, ^3J = 7.5 Hz), 8.58 (d, 2H, ^3J = 7.5 Hz). ^{13}C NMR (CD$_3$OD, 75 MHz): δ 23.1, 32.1, 57.0, 67.0, 122.3, 125.1, 125.9, 126.1, 139.7, 140.1, 149.0, 154.1, 155.5, 156.1, 168.0, 173.7, 176.4. FAB$^+$/MS: 572.5 ([LH$_4$ + H]$^+$, 100%). Anal. Calcd for $C_{29}H_{25}N_5O_8$·3HCl: C, 51.15; H, 4.14; N, 10.28. Found: C, 51.01; H, 4.43; N, 9.95.

Synthesis of the Complexes. [EuL(H$_2$O)]Na·4H$_2$O. LH$_4$·3HCl (60 mg, 88 μmol) was dissolved in a mixture of 30 mL of methanol and 30 mL of water. To this solution was added a mixture of EuCl$_3$·6H$_2$O (36 mg, 98 μmol) in 3 mL of methanol and 3 mL of water. The solution was heated to 70 °C for 1 h. After the mixture was cooled to room temperature, the pH was brought to 7.4 with a 5% NaOH solution in water. The solution was concentrated under reduced pressure until a precipitate appeared; THF was then added to complete precipitation. Upon centrifugation, [Eu**L**(H$_2$O)]Na·4H$_2$O (62 mg, 85%) was isolated as a beige powder. ^{1}H NMR (D$_2$O/CD$_3$OD, 200 MHz, all signals appear as broad singlets): δ −19.15 (1H), −16.70 (1H), −8.62 (1H), −8.22 (1H), −4.90 (1H), −4.31 (1H), −3.46 (1H), −2.46 (1H), 1.47 (1H), 4.14 (1H), 6.34 (1H), 7.37 (1H), 8.11 (1H), 8.42 (1H), 9.45 (1H), 9.95 (1H), 10.15 (1H), 11.81 (2H), 12.47 (1H). IR (KBr, cm^{-1}): 3420, 1619, 1574, 1460, 1384, 1274. Anal. Calcd for $C_{29}H_{21}NaN_5O_8Eu$·5H$_2$O: C,

(48) Perrin, D. D.; Armarego, W. L. F. *Purification of Laboratory Chemicals*, 3rd ed.; Pergamon Press: New York, 1988.
(49) Haas, Y.; Stein, G. *J. Phys. Chem.* **1971**, *75*, 3668.
(50) Nakamaru, K. *Bull. Chem. Soc. Jpn.* **1982**, *55*, 2697.
(51) Meech, S. R.; Phillips, D. *J. Photochem.* **1983**, *23*, 193.
(52) Roda, A.; Guardigli, M.; Pasini P. In *Bioluminescence and Chemiluminescence 2000*; Proceedings of the 11th International Symposium on Bioluminescence and Chemiluminescence; Case, J. F., Herring, P. J., Robison, B. H., Haddock, S. H. D., Kricka, L. J., Stanley, P. E., Eds.; World Scientific Publishing Co.: Singapore, 2001; p 493.

41.84; H, 3.75; N, 8.41. Found: C, 41.93; H, 3.62; N, 8.44. FAB$^+$/MS: 720.2 (80%), 722.2 (100%), [EuLH + H]$^+$.

[TbL(H$_2$O)]Na·3H$_2$O. L**H**$_4$·3HCl (40 mg, 59 μmol) was dissolved in a mixture of 30 mL of methanol and 30 mL of water. To this solution was added a mixture of TbCl$_3$·6H$_2$O (25 mg, 67 μmol) in 5 mL of methanol and 5 mL of water. The solution was heated to 70 °C for 1 h. After the mixture was cooled to room temperature, the pH was brought to 7.2 with a 1% NaOH solution in water. The solution was concentrated under reduced pressure until a precipitate appeared; THF was then added to complete precipitation. Upon centrifugation, the complex (46 mg, 95%) was isolated as a pale yellow powder. IR (KBr, cm^{-1}): 3428, 1592, 1574, 1466, 1416, 1387. Anal. Calcd for C$_{29}$H$_{21}$-NaN$_5$O$_8$Tb·4H$_2$O: C, 42.40; H, 3.56; N, 8.53. Found: C, 42.28; H, 3.31; N, 8.38. FAB$^-$/MS: 726.2 (30%, [TbL]$^-$), 668.2 (100%, [TbL − CH$_2$COONa]$^-$).

[GdL(H$_2$O)]Na·2H$_2$O. L**H**$_4$·3HCl (30 mg, 44 μmol) was dissolved in a mixture of 25 mL of methanol and 25 mL of water. To this solution was added a mixture of GdCl$_3$·6H$_2$O (19 mg, 51 μmol) in 5 mL of methanol and 5 mL of water. The solution was heated to 70 °C for 1 h. After being cooled to room temperature, the pH was brought to 7.5 with a 0.5% NaOH solution in water. The solution was concentrated under reduced pressure until a precipitate appeared; THF was then added to complete precipitation. Upon centrifugation, the complex (30 mg, 85%) was isolated as a pale yellow powder. IR (KBr, cm^{-1}): 3422, 1637, 1592, 1459, 1419, 1385. Anal. Calcd for C$_{29}$H$_{21}$GdNaN$_5$O$_8$·3H$_2$O: C, 43.44; H, 3.39; N, 8.73. Found: C, 43.35; H, 3.17; N, 8.55. FAB$^-$/MS: 725.2 (45%, [GdL]$^-$), 667.2 (100%, [GdL − CH$_2$COONa]$^-$).

[EuL*(H$_2$O)]. [EuL(H$_2$O)]Na·4H$_2$O (40 mg, 48 μmol) was suspended in 6 mL of DMSO. EDCI·HCl (12 mg, 63 μmol) and *N*-hydroxysuccinimide (7 mg, 61 μmol) were added, and the solution was stirred at room temperature for 66 h, resulting in the complete dissolution of the starting complex and in the formation of the product as a white precipitate. Upon centrifugation and drying at 50 °C under vacuum for 2 h, [EuL*(H$_2$O)]·4H$_2$O (31 mg, 71%) was isolated as a white powder. IR (KBr, cm^{-1}): 3420, 1739, 1629, 1573, 1459, 1384. Anal. Calcd for C$_{33}$H$_{25}$EuN$_6$O$_{10}$·5H$_2$O: C, 43.67; H, 3.89; N, 9.26. Found: C, 43.60; H, 3.80; N, 9.16. FAB$^+$/MS: 817.1, 819.1 ([EuL* + H]$^+$, 30%), 720.1, 722.1 ([EuL* − C$_4$H$_4$NO$_2$ + 2H]$^+$, 100%).

[TbL*(H$_2$O)]. [TbL(H$_2$O)]Na·3H$_2$O (50 mg, 61 μmol) was suspended in 5 mL of DMSO. EDCI·HCl (13 mg, 68 μmol) and *N*-hydroxysuccinimide (9 mg, 78 μmol) were added, and the solution was stirred at room temperature for 138 h, resulting in the complete dissolution of the starting complex and the formation of the product as a white precipitate. The product was isolated by centrifugation and washed with THF. An addition of THF to the mother liquor resulted in further precipitation of the product. Upon centrifugation and combination of the two precipitates, the activated complex (49 mg, 90%) was isolated as a white powder. IR (KBr, cm^{-1}): 3433, 1741, 1624, 1594, 1574, 1464, 1419, 1375. Anal. Calcd for C$_{33}$H$_{25}$N$_6$O$_{10}$Tb·4H$_2$O: C, 44.21; H, 3.71; N, 9.29. Found: C, 44.01; H, 3.42; N, 9.29. FAB$^+$/MS: 825.5 ([TbL* + H]$^+$, 100%), 726.2 ([TbL* − C$_4$H$_4$NO$_2$]$^+$, 15%).

[GdL*(H$_2$O)]. [GdL(H$_2$O)]Na·2H$_2$O (50 mg, 62 μmol) was suspended in 5 mL of DMSO. EDCI·HCl (15 mg, 78 μmol) and *N*-hydroxysuccinimide (9 mg, 78 μmol) were added, and the solution was stirred at room temperature for 48 h, resulting in the complete dissolution of the starting complex and the formation of the product as a white precipitate. The product was isolated by centrifugation and washed with THF. An addition of THF to the mother liquor resulted in further precipitation of the product. Upon centrifugation and combination of the two precipitates, the activated complex (45 mg, 82%) was isolated as a white powder. IR (KBr, cm^{-1}): 3435, 1741, 1623, 1573, 1465, 1420, 1376. Anal. Calcd for C$_{33}$H$_{25}$GdN$_6$O$_{10}$·3H$_2$O: C, 45.20; H, 3.56; N, 9.37. Found: C, 45.02; H, 3.18; N, 9.21. FAB$^+$/MS: 824.2 ([GdL* + H]$^+$, 100%), 726.5 ([GdL* − C$_4$H$_4$NO$_2$ + H]$^+$, 20%).

Synthesis of the Ln−BSA Conjugates (Ln = Eu or Tb). Bovine serum albumin (10 mg, 0.15 μmol) was dissolved in 500 μL of 0.05 M borate buffer (pH = 7.0), and [LnL*(H$_2$O)] (Ln = Eu or Tb, 3.7 mg, 4.5 μmol) was added to achieve a 30:1 label/protein reaction ratio. The solution was gently stirred at room temperature for 24 h, resulting in the complete dissolution of the activated lanthanide complex. The reaction mixture was concentrated to a low volume using a Centricon YM-30 centrifugal filter (Amicon, Millipore, Bedford, MA), and then ca. 1 mL of 0.01 M TRIS/HCl buffer (pH = 7.0) was added and the solution was concentrated again. The procedure was repeated until the filtrate does not present any detectable lanthanide luminescence to remove the unbound label.

Determination of the Stability Constant of the [EuL(H$_2$O)]Na Complex. Solutions containing [EuL(H$_2$O)]Na (5 μM in 0.01 M TRIS/HCl buffer, pH = 7.0, and 0.1 M NaCl) and different concentrations (10 μM to 10 mM) of EDTA were kept for 2 days at 60 °C and then at room temperature until the equilibrium was reached, which was confirmed by the absence of further changes in the absorption spectra. The concentrations of L**H**$_4$ and [EuL(H$_2$O)]Na were determined by means of UV−vis absorption spectroscopy, and then the ratio between the conditional stability constants for the formation of the [EuL(H$_2$O)]-Na and [Eu(EDTA)] complexes was determined as described by Wu et al.[39]